Long Term Performance of Alkali Activated Slag Concrete

by Arie Wardhono

Submission date: 12-Apr-2021 03:22PM (UTC+0700)
Submission ID: 1556944666
File name: C1c2_Artikel_Jurnal_Internasional_ACT.pdf (842.77K)
Word count: 4135
Character count: 21415

Technical report

Long Term Performance of Alkali Activated Slag Concrete

Arie Wardhono[1*], David W. Law[2] and Thomas C. K. Molyneaux[3]

A selected paper of ICCS13, Tokyo 2013. Received 30 October 2013, accepted 16 February 2015 doi:10.3151/jact.13.187

Abstract

This paper reports on an experimental program investigating the durability and mechanical properties of alkali activated slag concrete (AASC). The AASC was prepared using ground granulated blast furnace slag activated by high concentration alkali solution. The mechanical properties were determined by compressive strength and elastic modulus. The durability characteristics of AASC were measured using Ultrasonic Pulse Velocity (UPV) and permeable voids tests. The result showed that AASC developed a comparable strength to Portland Cement (PC) concrete over the short term. However, the material displayed an increase in voids, as well as a reduction of velocity over time. This could lead to the material displaying inferior performance over longer periods of time.

1. Introduction

The implementation of sustainable development in civil engineering has led to the use of a new material with low environmental impact. Ordinary Portland cement (PC) is the primary material in the production of traditional concrete. However, the manufacturing of PC has led to environmental concerns over the energy needed to produce the material, the depletion of the quarried resources and the production of CO_2. This has led to the use of slag, a waste product from the steel manufacturing process, as a cement replacement material due to its hydraulic properties, good durability and lower environmental impacts (Neville 2011).

Recent research has shown that it is possible to develop cement based solely on slag activated directly by alkali solution, without the presence of PC, utilizing Sodium Silicate (Na_2SiO_4), Sodium Hydroxide (NaOH), waterglass, or Sodium Carbonate (Na_2CO_3) as the activator (Bakharev *et al*. 1999; Roy 1999; Brough and Atkinson 2002; Law *et al*. 2012; Wardhono *et al*. 2012).

A major benefit of AASC is that the greenhouse gas emissions produced by AASC is reduced compared to PC, which depends on the limestone calcination process and produces around 5% of worldwide greenhouse emissions (Gartner 2004).

The development and properties of AASC have been studied in a number of papers. Some researchers have demonstrated the similarity of AASC to PC concrete over shorts periods of time in terms mechanical properties (Sakulich *et al*. 2009; Yang *et al*. 2009; Bondar *et al*. 2011; Bernal *et al*. 2012). The long term performance of AASC in terms of the micro-cracking and compressive strength development has been investigated by Collins and Sanjayan (2001). The authors found that the strength development tended to reduce. Using water sorptivity tests up to 360 days, they found that the reduction of strength could be attributed to the growing of the existence of a network of interconnected micro-cracks within the AAS concrete with increasing age.

This paper reports the results of experimental research on the long term performance of AASC up to the age of 540 days in terms of the materials durability and mechanical properties. The durability characteristics of the AASC were measured using Ultrasonic Pulse Velocity (UPV) and permeable voids tests, while the mechanical properties were assessed, in the form of compressive strength and elastic modulus.

2. Experimental procedures

2.1 Materials

(1) Cementitious materials

The primary raw materials used was ground granulated blast furnace slag (GGBS), a construction grade slag with a particle size distribution of 100% < 50 μm. The basicity coefficient was 0.81, which is in the preferred range for basicity as a starting material for alkali activated slag binder (Bakharev 2000). The hydration modulus was 1.5, which was selected to ensure good hydration properties (Chang 2003). **Table 1** presented the oxide composition analysis for GGBS. To ensure that the GGBS can be used successfully, the GGBS ratio of CaO/SiO_2 and Al_2O_3/SiO_2 should be between 0.5 to 2.0 and 0.1 to 0.6, respectively (Taling and Brandstetr 1989). In this trial the GGBS ratio for CaO/SiO_2 and Al_2O_3/SiO_2 were 0.98 and 0.39, respectively (**Table 1**).

Energy Dispersive X-ray (EDX) Spectroscopy using a Philip XL30SEM, operated at 20 keV, was employed to analyze the elemental composition at the surface of

[1]Lecturer, Dept. of Civil Engineering, Universitas Negeri Surabaya (Unesa), Surabaya, Indonesia.
*Corresponding author,
E-mail: arie.wardhono.unesa@gmail.com
[2]Lecturer, School of Civil, Environmental and Chemical Engineering, RMIT University, Melbourne, Australia.
[3]Associate Prof., School of Civil, Environmental and Chemical Engineering, RMIT University, Melbourne, Australia.

Table 1 Oxide composition of GGBS (%).

Components	AASC1	AASC2*
SiO_2	36.87	33.45
Al_2O_3	14.23	13.46
Fe_2O_3	0.32	0.31
CaO	36.00	41.74
MgO	5.05	5.99
K_2O	0.05	0.29
Na_2O	0.01	0.16
TiO_2	0.63	0.84
P_2O_5	0.36	0.12
Mn_2O_3	0.39	0.39
SO_3	6.08	6.08

Note: * Adam (2009)

GGBS sample. **Figure 1** shows the XRD difractograms of GGBS. The XRD analysis was recorded on a Bruker D4 Endeavour machine using a scanning rate of 1° from 6° to 90° 2-theta. The XRD diffractograms demonstrated that GGBS contained semi-crystalline and amorphous phases (indicated by the broad hump center at approximately 29° to 34° 2-theta) with low intensity peaks corresponding to gypsum (Yip *et al.* 2005).

(2) Alkaline activators

Alkaline activator solutions were formulated by blending Na_2SiO_4 with NaOH to achieve a Na_2O dosage of 5% and activator modulus (Ms) of 1.00. A Grade D Na_2SiO_4 with alkali modulus (AM) of 2 (Na_2O = 14.7% and SiO_2 = 29.4%) and a high concentration, 10 M NaOH in liquid form were used.

2.2 Mix proportions

Table 2 refers to the details of AASC mix proportions. Three AASC and one PC mix designs were investigated, designated AASC1, AASC2, AASC3, and Control. The mix design for AASC1 was developed from a previous project at RMIT University (Law *et al.* 2012). Liquid Na_2SiO_4 and NaOH were blended providing the alkali

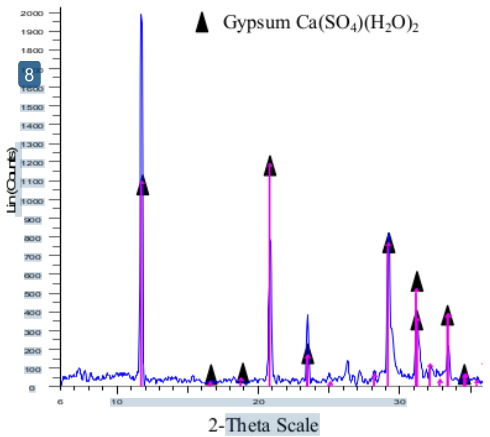

Fig.1 XRD analysis of GGBS samples.

Table 2 Mix proportion of AASC specimens (kg/m^3).

Materials	AASC1	AASC2*	AASC3**	Control*
OPC	NA	NA	NA	428
GGBS	415	415	400	NA
Fine aggregate	784	784	860	784
Coarse aggregate	1039	1039	860	1039
Sodium silicate	71	71	28	NA
Sodium hydroxide	46	46	84	NA
Water	136	136	156	222

Note: * Adam (2009) , ** Bernal et al. (2012)

modulus (mass ratio of SiO_2 to Na_2O) of 1.00. The concentration level of Na_2O is 5% by slag mass in the AAS mix. The design for each mix was for a 28-day strength of 40 ± 10 MPa. A water binder ratio (w/b) and water solid ratio (w/s) of 52% and 46% were used to prepare the AASC1 respectively.

As comparison, the data of alkali activated slag concrete (AASC2) and Portland Cement concrete (Control) from Adam (2009) at RMIT University have been used, as well as the data of alkali activated slag concrete derived from Bernall *et al.* (AASC3) mix design with Si/Al ratio of 3.60 (Bernal *et al.* 2012), which was close to Si/Al ratio of AASC1 = 2.59 and AASC2 = 2.48 (Adam 2009).

2.3 Specimen preparations

The mixing for AASC1 specimens was undertaken using a 25 liter concrete mixer. The mix was then poured into cylindrical molds (100 x 200 mm^2) for compressive strength, elastic modulus and permeable voids tests, as well as concrete block molds (200 x 200 x 100 mm^3) for UPV testing, and vibrated. The specimens were cured at 20 degree C in water for 6 days after de-molding and then left at room temperature prior to testing.

2.4 Testing specimen

The mechanical properties of AASC1 samples were determined by compressive strength and elastic modulus. Compressive strength was performed on a Universal Testing Machine, UH-F500 kNI, Shimadzu, under a load control regime with loading rate of 20 MPa/min (AS 1012.9 1999). The static elastic modulus was determined by subjecting cylinder specimen to uniaxial compression with a loading rate of 15 MPa/min (AS 1012.17 1997) and measuring the deformation using LVDT equipment. A series of readings were taken and the stress-strain relationship was established. Three cylinders were tested for each data point.

The characteristics of AASC1 were tested using Ultrasonic Pulse Velocity (UPV), voids and density tests. The UPV test was carried out to determine the bulk property of AASC1 (ASTM C597-02 2003). It was measured with a pulse of longitudinal vibration energy produced by an electro-acoustical transducer and received by another transducer after travelling a known path. The transit time (T) and the pulse velocity (V) was measured and calculated. The permeable voids test was undertaken to determine the amount of voids of the

AASC1 specimen (ASTM C642-97 2003), as well as to identify the possibility of micro-cracks developments on AASC1 concrete specimen. The density test was performed to identify the mass per unit volume of the AASC1 specimens using the rapid measuring method (AS 10.12.12.1 1998). Instead of using the saturated surface dry (SSD) condition for the specimen, the dry condition was applied to determine the density development of AASC1 specimen in regards to the possibility of micro-cracks developments. AASC1 specimens were tested at 28, 90, 180, 360 and 540 days after casting.

3. Results and discussions

3.1 Strength development

Table 3 gives the compressive strength results reported for the AASC1 specimen. The AASC demonstrated a comparable initial strength of 39.47 MPa with the PC concrete at 28 days. A slight increase in the AASC1 strength was also observed up to 90 days age. However, beyond that, the compressive strength of the AASC1 did not display any increase with time, but shows a slight reduction in strength. It was observed that the highest strength of AASC1 of 41.57 MPa was achieved at 90 days. However, this strength reduced to 41.26 MPa, 40.43 MPa and 38.31 MPa at 180, 360 and 540 days, respectively.

Figure 2 shows a comparable initial strength of AASC1, AASC2 and AASC3 specimens with the PC concrete. The, AASC3 had a lower initial strength compared to AASC1 and AASC2. However, the strength development of AASC3 increased significantly from 28 to 90 days. Indeed all specimens showed some increase in strength from 28 to 90 days. While the OP concrete showed a further appreciable increase with time to 180 days the AASC3 showed only a marginal further increase to 180 days and the AASC1 actually showed a small decrease. The AASC1 showed further reductions from 180 to 360 and from 360 to 540 days.

The strength development of the AASC specimens has been identified as being affected by the ratio of SiO_2 to Al_2O_3 (Si/Al ratio) (Sakulich *et al*. 2010; Bernal *et al*. 2012). **Figure 3** shows the strength development of AASC1, AASC2 and AASC3 with Si/Al ratio of 2.48, 2.59 and 3.60 respectively. The high Si/Al ratio tended to reduce the early age reaction of the AASC mix. The early age reactions in the AASC system are fundamentally based on the alkali mediated dissolution mechanism (Wang and Scrivener 1995). Hence, the high ratio of Si/Al, in AASC3, reduced the alkalinity through the deprotonation of hydrate silica molecules and the consumption of Na by the formation alumino silicate reaction products (Bernal *et al*. 2012), and so delayed the early age reactions in the AASC3, resulting in lower initial strengths.

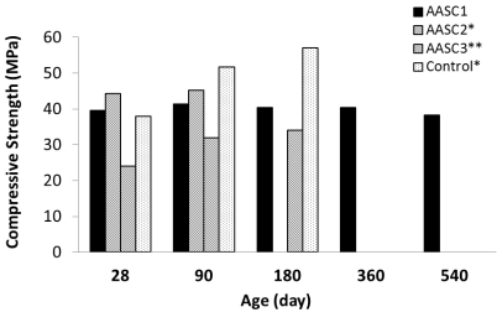

Note: * Adam (2009), ** Bernal *et al*. (2012)

Fig.2 AASC strength development.

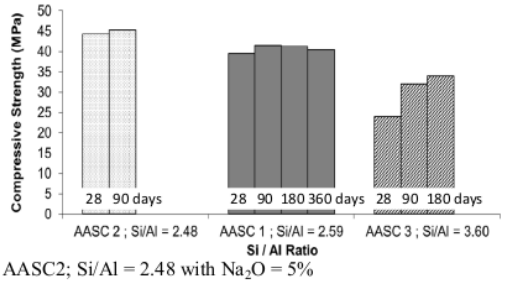

AASC2; Si/Al = 2.48 with Na_2O = 5% and Ms = 1 (Adam 2009)
AASC1; Si/Al = 2.59
AASC3; Si/Al = 3.60 with 100% GBFS (Bernal et al. 2012)

Fig.3 Effect of Si/Al ratio.

3.2. Elastic modulus development

The elastic modulus is a property of concrete that expresses the ratio between a certain range of unit stress and unit elongation within the elastic limit. A higher elastic modulus will represent a better quality of concrete specimen. The elastic modulus of AASC1 (based on experimental test in accordance with AS 1012.17-1997, the PC concrete (based on article 3.1.2(a)(ii) in accordance with AS 3600-2009 and the AAS (based on equation formula proposed by Ng & Foster (Concrete Institute of Australia 2011) are presented in **Fig. 4**.

The elastic modulus of ordinary concrete is affected by the modulus of aggregate and mortars. For PC concrete, the relationship between the elastic modulus and compressive strength followed a positive linear relation (ACI 318M-08 2008). A similar pattern was also shown for the Alkali Activated Slag (AAS) model proposed by Ng & Foster, which demonstrated a lower elastic modulus than PC concrete (Ng and Foster 2008). Based on these, it can be inferred that the elastic modulus for

Table 3 AASC1 test results and standard deviation.

AASC1	28 days	90 days	180 days	360 days	540 days
Compressive strength (MPa)	39.47 ± 1.11	41.57 ± 1.18	41.26 ± 2.06	40.43 ± 0.25	38.31 ± 1.91
Elastic modulus (MPa)	25689 ± 683	21413 ± 2446	18093 ± 544	16545 ± 1629	15397 ± 935

PC concrete and geopolymer mortar will not change in long term performance (ACI 318M-08 2008; Ng and Foster 2008; Concrete Institute of Australia 2011). The short term behavior of AASC1 at 28 days age showed a comparable elastic modulus with that of AAS and PC, which indicates that the equation proposed Ng & Foster could be applied. However, the elastic modulus of AASC1 subsequently showed a decline with time, **Fig. 4**, indicating the model does not correctly predict the performance of the AAS in the long term. The long term trend being the opposite of that of standard PC concrete, contrary to the ACI model prediction. This would also indicated that the interaction between the AAS paste and the aggregates at the aggregate/paste interface, the principal factor that affecting the modulus of elasticity, becomes brittle. Overall a decrease in elastic modulus of 40.1% is observed between 28 and 540 days.

3.3 Density development

The UPV can be related to the bulk density of the concrete. A higher density material will enable the ultrasonic wave to move through the medium more quickly, and hence higher velocity indicates a denser material. For PC concrete, previous research has shown an increase in velocity with increasing strength (Bungey 1980). This is due to the hydration reaction in concrete resulting in more solid material, allowing the ultrasonic pulse to travel at a higher velocity through the concrete. **Figure 5** showed a significant decrease for AASC1 velocity with time. Density measurements obtained directly by mass and volume measurements of the specimens, **Fig. 6**, showed a reduction in density with time.

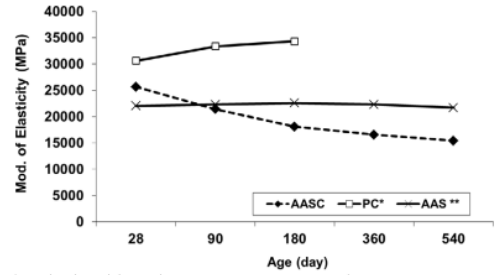

* Calculated based on AS 3600-2009 section 3.1
** Calculated based on Ng and Foster model (Ng and Foster 2008)

Fig.4 AASC1 elastic modulus development.

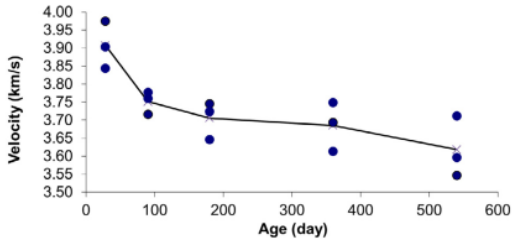

Fig.5 Velocity vs time for AASC1.

The velocity would be expected to increase with a reduction in density but decrease with a reduction in elastic modulus. The density of AASC1 has been related to the fineness of the slag precursor (Diaz-Loya *et al.* 2011). The reduction in density could be explained by the fact that during the mixing of AASC1, the activator solution demand rose as the fineness decreased due to the need to fill larger voids among coarser slag particles to achieve a workable material. A higher proportion of activator solution (Collins and Sanjayan 2001; Sakulich *et al.* 2010) might cause the overall density of the AASC1 to decrease which could also lead to the decrease of elasticity modulus observed.

3.4 Permeable voids development

The permeable voids of concrete are associated with the amount of the empty space in concrete. Lower permeable voids suggest a higher density material. However, higher voids indicate a high quantity of empty space in material and the possibility of micro-cracks. **Figure 7** showed an increase of porosity measurement for the AASC1 specimen of 0.96% and 1.40% at the age 360 and 540 days, respectively. The development of permeable voids also corroborated the behavior exhibited by the velocity and density development shown in **Figs. 5** and **6**, respectively. The increase in permeable voids coupled with the decrease in density and velocity, as well as the reduction of elastic modulus was attributed to the formation of the micro-cracks. Micro-cracks were observed at the interface between aggregate and mortar and micro-cracks were also found on the border of C-S-H gel with un-reacted silicate, **Fig. 8**. This micro-cracking is attributed to the formation of an unstable gel phase during drying mechanism within the activated

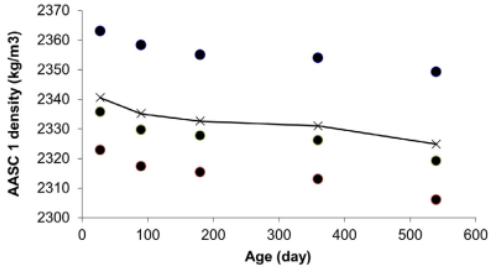

Fig. 6 Density vs time for AASC1.

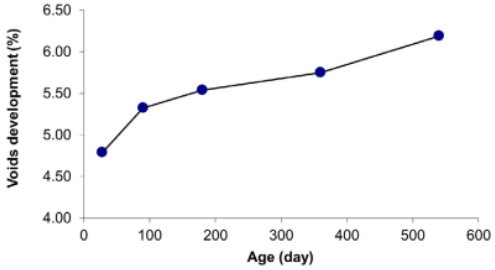

Fig. 7 Permeable voids vs time for AASC1.

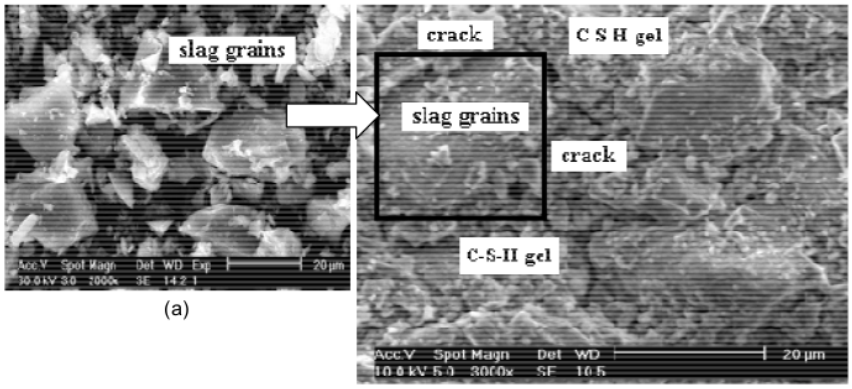

(a)

(b)

Fig. 8 Slag grains (a) and micro-cracks occurrence in AASC1 specimen (b).

slag paste which leads to a number of breaks in the particle to particle bonds throughout the gel structure. This phenomenon has previously been observed by Collins and Sanjayan where micro-cracking has become progressively larger and continuous with increasing age followed by crack width growth (Collins and Sanjayan 2001).

Overall the results show that AASC displays similar performance characteristics to PC concrete in the short term (90 days), but over the long term the performance characteristics diverge significantly. The AASC displays a reduction in compressive strength, density and UPV and an increase in porosity in the longer term (360-540 days). This is hypothesized as being due to the formation and growth of micro-cracks with time.

4. Conclusions

The following conclusions may be drawn based on this study:

(1) The early strength of AASC has a comparable strength with PC concrete. However at a later age the strength of AASC is less than that of PC concrete.

(2) The ratio of SiO_2 to Al_2O (Si/Al ratio) affects the strength development of AASC. A higher Si/Al ratio was observed to delay the early age reaction of AASC.

(3) The elastic modulus of AASC is comparable to that of PC concrete at 28 days. However, the performance of the AASC tends to decline over the long term. The relationship between the elastic modulus and the compressive strength followed a negative linear relationship for the AASC.

(4) The reduction of elastic modulus of AASC over time is accompanied by a reduction of density.

(5) The reduction of density of AASC might be caused by the occurrence of micro-cracks which are becoming progressively larger and more continuous with increasing time.

(6) The increase of permeable voids over periods of time also indicated the micro-cracks width growth.

(7) The AASC demonstrates good short term behavior, however the use of AASC over the long term for structural engineering components needs to be further studied on account of the reduction of the density and elastic modulus, as well as the increase of the permeable voids.

Acknowledgment

The authors would like to express their sincere thanks to Directorate General of Higher Education (DIKTI) of Indonesian government for providing the scholarship for this research project. Materials support from the Independence Cement Pty. Ltd. Australia and PQ Australia for carrying out this research project is gratefully acknowledged. The authors also acknowledge the facilities, and the scientific and technical assistance, of the Australian Microscopy & Microanalysis Research Facility at the RMIT Microscopy & Microanalysis Facility, at RMIT University

References

ACI 318M-08, (2008). "*Building code requirements for structural concrete (ACI 318M-08) and Commentary.*" Reported by ACI Committee 318. American Concrete Institute. Farming Hills, MI 48331, U.S.A.

Adam, A. A., (2009). "*Strength and durability properties of alkali-activated slag and fly ash-based geopolymer concrete.*" Dissertation. School of Civil, Environment and Chemical Engineering, RMIT University, Melbourne, Australia.

ASTM C597-02, (2003). "*Standard test method for pulse velocity through concrete.*" ASTM International, USA.

ASTM C642-97, (2003). "*Standard test method for density, absorption, and voids in hardened concrete.*" ASTM International, USA.

AS 1012.9, (1999). "*Methods of testing concrete. Method 9: Determination of the compressive strength*

of concrete specimens." Australian Standard Association, Australia.

AS 1012.17, (1997). "*Methods of testing concrete. Method 17: Determination of the static chord modulus of elasticity and Poisson's ratio of concrete specimens*." Australian Standard Association, Australia.

AS 10.12.12.1, (1998). "*Methods of testing concrete. Method 12.1: Determination of mass per unit volume of hardened concrete - Rapid measuring method*." Australian Standard Association, Australia.

Bakharev, T., Sanjayan, J. G. and Cheng, Y. B., (1999). "Alkali activation of Australian slag cements." *Cement and Concrete Research*, 29, 113-120.

Bakharev, T., (2000). "Alkali activated slag concrete: Chemistry, microstructure and durability." Dissertation. Monash University, Melbourne, Australia.

Bernal, S. A., Gutierrez, R. M. d. and Provis, J. L., (2012). "Engineering and durability properties of concretes based on alkali-activated granulated blast furnace slag/metakaolin blends." *Construction and Building Materials*, 33, 99-108.

Bondar, D., Lynsdale, C. J., Milestone, N. B., Hassani, N. and Ramezanianpour, A. A., (2011). "Engineering properties of alkali-activated natural pozzolan concrete." *ACI Materials Journal*, Title no. 108-M08, January - February,

Brough, A. R. and Atkinson, A., (2002). "Sodium silicate-based, alkali-activated slag mortars. Part I. Strength, hydration and microstructure." *Cement and Concrete Research*, 32, 865-879.

Bungey, J. H., (1980). "The validity of ultrasonic pulse velocity testing of in-place concrete for strength." *NDT International*, December, 296-300.

Chang, J. J., (2003). "A study on the setting characteristics of sodium silicate-activated slag pastes." *Cement and Concrete Research*, 33, 1005-1011.

Collins, F. and Sanjayan, J. G., (2001). "Microcracking and strength development of alkali activated slag concrete." *Cement and Concrete Composites*, 23, 345-352.

Concrete Institute of Australia, (2011). "Recommended practice geopolymer concrete." Sydney. New South Wales. Australia, Concrete Institute of Australia.

Diaz-Loya, E. I., Allouche, E. and Vaidya, S., (2011). "Mechanical properties of fly-ash-based geopolymer concrete." *ACI Materials Journal*, Technical Paper, Title no. 108-M32, May - June, 300-306.

Gartner, E., (2004). "Industrially interesting approaches to 'low-CO_2' cements." *Cement and Concrete Research*, 34, 1489-1498.

Law, D.W., A. A. Adam, T. C. K. Molyneaux, and Patnaikuni, I., (2012). "Durability assessment of alkali activated slag (AAS) concrete." *Materials and Structures*, 45, 1425-1437.

Neville, A. M., (2011). "*Properties of Concrete*" 5th ed. Harlow, England; New York. Pearson.

Ng, T. S. and Foster, S. J. (2008) Development of high performance geopolymer concrete. In: Future in Mechanics of Structures and Materials (The 20th ACMSM), Toowoomba. Australia.

Roy, D. M., (1999). "Alkali-activated cements: Opportunities and challenges." *Cement and Concrete Research*, 29, 249-254.

Sakulich, A. R., Anderson, E., Schauer, C. and Barsoum, M. W., (2009). "Mechanical and microstructural characterization of an alkali-activated slag/limestone fine aggregate concrete." *Construction and Building Materials*, 23, 2951-2957.

Sakulich, A. R., Anderson, E., Schauer, C. L. and Barsoum, M. W., (2010). "Influence of Si:Al ratio on the microstructural and mechanical properties of a fine-limestone aggregate alkali-activated slag concrete." *Materials and Structures*, 43, 1025-1035.

Taling, B. and Brandstetr, J., (1989). "Present state and future of alkali activated slag concretes." *American Concrete Institute*, 114, 1519-1546.

Wang, S. D. and Scrivener, K. L., (1995). "Hydration products of alkali activated slag cement." *Cement and Concrete Research*, 25 (3), 561-571.

Wardhono, A., Law, D. W. and Molyneaux, T. C. K., (2012). "Strength of alkali activated slag and fly ash-based geopolymer mortar." In: Pproceedings of Microstructural-related Durability of Cementitious Composites, Microdurability 2012, Amsterdam, Netherlands. RILEM Publications.

Yang, K. H., Song, J. K., Lee, K .S. and Ashour, A. F., (2009). "Flow and compressive strength of alkali-activated mortars." *ACI Materials Journal*, January - February, 50-58.

Yip, C. K., Lukey, G .C. and Deventer, J. S. J. v., (2005). "The coexistence of geopolymeric gel and calcium silicate hydrate at the early stage of alkaline activation." *Cement and Concrete Research*, 35, 1688-1697.

Long Term Performance of Alkali Activated Slag Concrete

ORIGINALITY REPORT

13%	10%	8%	3%
SIMILARITY INDEX	INTERNET SOURCES	PUBLICATIONS	STUDENT PAPERS

PRIMARY SOURCES

1	Arie Wardhono, David W. Law, Thomas C.K. Molyneaux. "Flexural Strength of Low Calcium Class F Fly Ash-Based Geopolymer Concrete in Long Term Performance", Materials Science Forum, 2016 Publication	3%
2	core.ac.uk Internet Source	3%
3	Submitted to University College London Student Paper	2%
4	demo.webdefy.com Internet Source	2%
5	C.K. Yip, G.C. Lukey, J.S.J. van Deventer. "The coexistence of geopolymeric gel and calcium silicate hydrate at the early stage of alkaline activation", Cement and Concrete Research, 2005 Publication	1%
6	vww.mrfreebook.com Internet Source	1%

7	invenio.itam.cas.cz Internet Source	1%
8	www2.gov.bc.ca Internet Source	1%

Exclude quotes	On	Exclude matches	< 1%
Exclude bibliography	On		